Effects of Temperature on the Kinetics of the Gated Electron-Transfer Reaction between Zinc Cytochrome *c* and Plastocyanin. Analysis of Configurational Fluctuation of the Diprotein Complex[†]

Maja M. Ivković-Jensen and Nenad M. Kostić*

Department of Chemistry, Iowa State University, Ames, Iowa 50011

Received July 3, 1996; Revised Manuscript Received September 16, 1996[⊗]

ABSTRACT: This is a study of the effects of temperature (in the range 273.3−307.7 K) and of ionic strength (in the range 2.5−100 mM) on the kinetics of photoinduced electron-transfer reaction ^{3}Zncyt/pc(II) → Zncyt$^+$/pc(I) within the electrostatic complex of zinc cytochrome *c* and cupriplastocyanin at pH 7.0. In order to separate direct and indirect effects of temperature on the rate constants, viscosity of the solutions was fixed, at different values, by additions of sucrose. The activation parameters for the reaction within the preformed complex, at the low ionic strength, are $\Delta H^{\ddagger} = 13 \pm 2$ kJ/mol and $\Delta S^{\ddagger} = -97 \pm 4$ J/K mol. The activation parameters for the reaction within the encounter complex, at the higher ionic strength, are $\Delta H^{\ddagger} = 13 \pm 1$ kJ/mol and $\Delta S^{\ddagger} = -96 \pm 3$ J/K mol. Evidently, the two complexes are the same. The proteins associate similarly in the persistent and the transient complex, i.e., at different ionic strengths. In both complexes, however, electron transfer is gated by a rearrangement, as previous studies from this laboratory showed. Changes in the solution viscosity modulate this rearrangement by affecting $\Delta H^{\ddagger}$, not $\Delta S^{\ddagger}$. The activation parameters are analyzed by empirical methods. The thermodynamic parameters ΔH and ΔS for the formation of the complex Zncyt/pc(II) are determined and related to changes in hydrophilic and hydrophobic surfaces upon protein association in three configurations. A difference between the values of ΔH for the configuration providing optimal electronic coupling between the redox sites and the configuration providing optimal docking equals the experimental value $\Delta H^{\ddagger} = 13$ kJ/mol for the rearrangement of the latter configuration into the former. Enthalpy of activation may reflect a change in the character of the exposed surface as the diprotein complex rearranges. Entropy of activation may reflect tightening of the contact between the associated proteins.

Various metalloproteins act as redox enzymes and electron carriers in respiration and photosynthesis, metabolism of nonmetals, detoxification of harmful compounds, and other processes of life. Biological functions of metalloproteins can be understood only if their interactions and reactions are understood at the molecular level. The required chemical studies are best made with well-characterized, small proteins and their pairs (Hoffman et al., 1991; Mauk, 1991; Pelletier & Kraut, 1992; Chen et al., 1992, 1994; McLendon, 1991a,b; McLendon & Hake, 1992; Zhou & Hoffman, 1994; Zhou et al., 1995; Therien et al., 1991; Winkler & Gray, 1992; Kostić, 1991). Despite vigorous current research, mechanisms of electron-transfer reactions of metalloproteins are only partially understood.

The heme protein cytochrome *c* (Pettigrew & Moore, 1987; Moore & Pettigrew, 1990; Scott & Mauk, 1996) and the blue copper protein plastocyanin (Redinbo et al., 1994; Gross, 1993; Sykes, 1991a,b), designated cyt and pc,[1] are nicely suited to kinetic and mechanistic studies even though they are not physiological partners. Their three-dimensional structures in both oxidized and reduced states and in both crystal and solution are known in detail, and their active sites have been thoroughly examined by spectroscopic, electrochemical, and quantum-chemical methods.

A pair of metalloproteins can form multiple complexes in solution (Willie et al., 1992; Mauk et al., 1994; Zhou & Hoffman, 1994; Northrup et al., 1988; Wendoloski et al., 1987; Rodgers et al., 1988; Burch et al., 1990; Wallin et al., 1991; McLendon et al., 1993; Roberts et al., 1991; Nocek et al., 1991; Harris et al., 1994), and an orientation that is optimal for recognition and binding need not be optimal for the subsequent reaction. The rate of the intracomplex electron-transfer reaction may be limited by the rate of rearrangement; in such a case the reaction is gated (Nocek et al., 1991; Feitelson & McLendon, 1991; Walker & Tollin, 1992; Sullivan et al., 1992; Hoffman & Ratner, 1987, 1988; Hoffman et al., 1990; Brunschwig & Sutin, 1989). The phenomenon of gating is not limited to electron-transfer reactions, and it may be common in proteins.

In the chemical equations below the slash mark represents protein association (diprotein complex), and the Roman numerals are the oxidation states of iron and copper. Studies in our laboratory and in other laboratories of the unimolecular reaction in eq 1 (Peerey & Kostić, 1989; Peerey et al., 1991; Meyer et al., 1993) and of the bimolecular reaction in eq 2 (Modi et al., 1992a) showed that ferrocytochrome *c* reduces cupriplastocyanin from the acidic patch, but not from the initial binding site within this broad patch. Similar conclusions were reached about the reactions between ferrocyto-

[†] This work was supported by the National Science Foundation through Grant MCB-9222741.

[⊗] Abstract published in *Advance ACS Abstracts,* November 15, 1996.

[1] Abbreviations: b_5, cytochrome b_5; b_5(II), ferrocytochrome b_5; b_5-(III), ferricytochrome b_5; cyt, cytochrome *c*; pc, plastocyanin; pc(I), cuproplastocyanin; pc(II), cupriplastocyanin; Sncyt, tin(IV) cytochrome *c*; ^{3}Sncyt, triplet (excited) state of tin(IV) cytochrome *c*; Sncyt$^+$, cation radical of tin(IV) cytochrome *c*; Zncyt, zinc cytochrome *c*; ^{3}Zncyt, triplet (exited) state of zinc cytochrome *c*; Zncyt$^+$, cation radical of zinc cytochrome *c*.

S0006-2960(96)01608-X CCC: $12.00

chrome *f* and cupriplastocyanin analogous to those in eqs 1 and 2 (Qin & Kostić, 1992, 1993; Modi et al., 1992b).

$$\text{cyt(II)/pc(II)} \rightarrow \text{cyt(III)/pc(I)} \quad (1)$$

$$\text{cyt(II)} + \text{pc(II)} \rightarrow \text{cyt(III)} + \text{pc(I)} \quad (2)$$

$$^3\text{Zncyt/pc(II)} \rightarrow \text{Zncyt}^+\text{/pc(I)} \quad (3)$$

$$\text{Zncyt}^+\text{/pc(I)} \rightarrow \text{Zncyt/pc(II)} \quad (4)$$

$$^3\text{Zncyt} + \text{pc(II)} \rightarrow \text{Zncyt}^+ + \text{pc(I)} \quad (5)$$

$$\text{Zncyt}^+ + \text{pc(I)} \rightarrow \text{Zncyt} + \text{pc(II)} \quad (6)$$

$$^3\text{Sncyt/pc(II)} \rightarrow \text{Sncyt}^+\text{/pc(I)} \quad (7)$$

$$^3\text{Zncyt}/b_5\text{(III)} \rightarrow \text{Zncyt}^+/b_5\text{(II)} \quad (8)$$

$$\text{cyt(III)/pc(II)} + {}^3\text{Zncyt} \rightarrow \text{cyt(III)/pc(I)} + \text{Zncyt}^+ \quad (9)$$

Kinetics and mechanism of the necessary rearrangements of the diprotein complex have been studied with derivatives of cytochrome *c* containing zinc(II) or tin(IV) in the heme (Zhou & Kostić, 1991a,b, 1992a,b,c, 1993a,b; Qin & Kostić, 1994, 1996; Kostić, 1996). The thermal interprotein electron-transfer reactions in eqs 1 and 2 are initiated by external reduction or oxidation of one of the proteins. Since the temperature change would affect both the initiation reaction and the subsequent reaction of interest, the interpretation of the temperature effects on kinetics would be ambiguous. The photoinduced reactions in eqs 3−9, however, are fast and do not require additional redox agents in solution. In them, the interprotein electron-transfer reaction of interest is triggered by a photon. The reactions in eqs 3, 5, 7, 8, and 9, in which the triplet state is the electron donor (reductant), are termed forward reactions. Those in eqs 4 and 6, in which the cation radical of zinc cytochrome *c* is the electron acceptor (oxidant), are termed back reactions. The reactions in eqs 1 and 2, which have a small electromotive driving force, are truly redox reactions—the rate-limiting step in them is electron transfer. The reactions in eqs 3, 5, 7, and 8, which have large electromotive driving forces, are gated by a rearrangement process independent of this driving force. Because the electron transfer in these photoinduced reactions is faster than the rearrangement, the latter is the rate-limiting step, the one actually observed in kinetic experiments.

The nature of this interesting rearrangement was studied both experimentally and theoretically (Zhou & Kostić, 1992a, 1993b; Qin & Kostić, 1994; Ullmann & Kostić, 1995). Quantitative analysis of viscosity effects on kinetics of the reaction in eqs 3, 7, and 8 showed the rearrangement to be configurational fluctuation of the diprotein complex, a process during which the donor and the acceptor remain docked in the same general orientation but wiggle with respect to each other. A theoretical analysis of electron-transfer paths between the heme and blue copper sites in various configurations of the cyt(II)/pc(II) complex confirmed the experimental findings (Ullmann & Kostić, 1995). The configuration that optimizes the surface interactions does not optimize the heme−copper electronic coupling. Motions of the cytochrome *c* molecule, whose basic patch explores the area within or near the acidic patch in plastocyanin, enhance the electronic coupling. The configurational fluctuation thus improves the intrinsic electron-transfer reactivity.

These previous studies in our laboratory answered some, but not nearly all, questions concerning the dynamic motions that gate the photoinduced reactions. In this study we collect data at constant pH, four constant viscosities, five ionic strengths, and seven temperatures. We report systematic kinetic experiments and analyze the energetics of activation. This analysis indicates a possible pathway for the rearrangement.

MATERIALS AND METHODS

Chemicals. Distilled water was demineralized to a resistivity greater than 17 MΩ·cm. Sucrose and chromatography gels (CM Sephadex C-50, Sephadex G-25 and G-75, and Sephadex DEAE A-25) were purchased from Sigma Chemical Co. Hydrogen fluoride, nitrogen, and ultrapure argon were purchased from Air Products Co. All other chemicals were purchased from Fischer Chemical Co.

Buffers. All buffers were made fresh from NaH_2PO_4 and Na_2HPO_4 and had pH 7.0 at 293 K. The ionic strength (μ) of these salts was 2.5 or 10.0 mM. It was adjusted to 20.0, 30, or 100 mM by addition of NaCl to the phosphate buffer having the intrinsic ionic strength of 10.0 mM. Since all the buffers contained the same salts and had the same pH, it is enough to specify their ionic strength.

Viscosity. The absolute viscosity (η) of water and of aqueous solutions of sucrose at different temperatures were read and interpolated from tables (ISCO, 1982; Barber, 1966; *CRC Handbook of Chemistry and Physics; CRC Handbook of Biochemistry and Molecular Biology*). The relative viscosity (η/η_0) of pure and sucrose-containing buffers was measured with a thermostated glass viscometer; the absolute error was ±0.05 cp. Given $\eta_0 = 1.002$ cp, the absolute viscosity was calculated. The viscosity of buffered protein solutions was raised by adding calculated amounts of a 70% w/w sucrose solution in the buffer of desired ionic strength. These additions were made at each temperature anew, for precise control of viscosity.

Proteins. Horse-heart cytochrome *c* was purchased from Sigma Chemical Co. The iron-free (so-called free-base) form was made, purified, and reconstituted with zinc(II) by a modification (Ye et al., 1997) of the original procedure (Vanderkooi & Erecińska, 1975; Vanderkooi et al., 1976). The product, zinc cytochrome *c*, was handled at 4 °C, in the dark. Two of the criteria of purity were the absorbance ratios $A_{423}/A_{549} > 15.4$ and $A_{549}/A_{585} < 2.0$. The third was the rate constant for natural decay of the triplet state, $k_d < 110\ s^{-1}$; it was checked before each series of kinetic experiments. Plastocyanin was isolated from French bean by a standard procedure (Milne & Wells, 1970) and purified repeatedly by gel-filtration chromatography on Sephadex G-25 and G-75 columns and by an ion exchange chromatography on a Sephadex DEAE A-25 column; the criterion of purity was the absorbance quotient $A_{278}/A_{597} < 1.20$. Both proteins were desalted, transferred into a 2.5 mM phosphate buffer at pH 7.0, and stored in liquid nitrogen. Before each series of kinetic experiments plastocyanin was treated with a small excess of dissolved $K_3[Fe(CN)_6]$, which was removed with Centricon ultrafiltration cells. Concentrations of the two proteins were determined from their UV−vis spectra, on the basis of the known absorptivities: $\epsilon_{423} = 2.43 \times 10^5\ M^{-1}$

cm^{-1} for zinc cytochrome *c* (Vanderkooi et al., 1976) and $\epsilon_{597} = 4500\ M^{-1}\ s^{-1}$ (Milne & Wells, 1970) for cupriplastocyanin.

Flash Kinetic Spectrophotometry. So-called laser flash photolysis on the microsecond scale was done with a standard apparatus (Zhou & Kostić, 1991a,b, 1992b, 1993a,b). Argon was passed first through water and then through the solution to be deaerated. Buffers were deaerated by vigorous bubbling of argon for at least 30 min, at room temperature. The required volume of a buffer was further deaerated in a 10-mm cuvette for 30 min. Next, the cell jacket was connected to a 30-L circulating bath Forma 2067, which maintained the temperature to ±0.2 °C. The actual temperature in the cell was calibrated with an Omega HH82 digital thermometer and was known with a precision of ±0.1 °C. The temperature range was 0.1−34.5 °C, or 273.3−307.7 K. After the temperature of the buffer was adjusted, other solutions were added. Viscosity was adjusted with sucrose solutions in the required buffers; the concentration of zinc cytochrome *c* was made 10.0 μM; and the concentration of cupriplastocyanin was varied between 2.00 and 30.0 μM. After each exposure to air, the solution in the cuvette was gently deaerated for 10−15 min. Determinations of k_d in control experiments proved this deaeration to be thorough. Formation and decay (natural or by quenching) of the triplet state, ^{3}Zncyt, were monitored at 460 nm. Its concentration depended on the intensity of the laser pulse and was ca. 1.0 μM, much lower than the cupriplastocyanin concentration. Conditions for the kinetics of pseudo-first-order were thus satisfied. At each set of conditions (temperature, viscosity, ionic strength, and cupriplastocyanin concentration) 5−20 laser pulses were delivered. Error bars in the figures enclose all of the corresponding experimental values. The change of absorbance with time was analyzed with kinetic software from OLIS, Inc., and with the fitting program SigmaPlot 1.02, from Jandel Scientific Co. The standard errors of fitting, which are given in the tables, are computed by dividing the standard deviation by the square root of the number of measurements.

Protein Surface Areas. The surface area accessible to water was defined as usual (Connolly, 1983) and computed with the program package QUANTA 4.0. The radius of the probe sphere was 1.4 Å, and the dot density was 20 $Å^{-1}$. We examined cytochrome *c* (Takano & Dickerson, 1981), plastocyanin (Guss & Freeman, 1983), and three configurations of the electrostatic complex between these two proteins. These configurations were designated maximum-overlap (max ov); maximum-overlap, rotated (max ov rot); and northern equatorial (n/eq) in the original study (Roberts et al., 1991) and afterward (Ullmann & Kostić, 1995). For the sake of consistency, we retain these designations and abbreviations.

RESULTS

Natural Decay of the Triplet State, ^{3}Zncyt. The rate constant k_d for the simple process in eq 10 was obtained from fittings of the traces to the monoexponential eq 11.

$$^3\text{Zncyt} \xrightarrow{k_d} \text{Zncyt} \tag{10}$$

$$\Delta A = a \exp(-k_d t) \tag{11}$$

This rate constant is independent of protein concentration, ionic strength in the interval 2.5 mM ≤ μ ≤ 100 mM, and wavelength; independent of viscosity through 8.40 cp and slightly lowered at 16.00 cp; and dependent on temperature, as follows: 80 ± 3 and 180 ± 15 s^{-1} at 273.3 and 307.7 K, respectively. See Supporting Information, Figure S1. Although this temperature dependence is relatively small, we did not exceed 302.9 K in the experiments that follow. This precaution improved the accuracy of the kinetic results.

Although k_d does not depend on ionic strength, stability of zinc cytochrome *c* does, slightly. Bubbling with argon for as long as 5 h at low and intermediate ionic strengths (20.0 mM ≤ μ ≤ 100 mM) did not affect the natural decay; k_d remained 110 s^{-1}. This prolonged bubbling at the lowest ionic strengths, however, caused a slight increase in the decay rate: 125 s^{-1} at 10.0 mM and 140 s^{-1} at 2.5 mM. For this reason, deaeration in subsequent experiments lasted at most 3 h. This time proved more than sufficient for obtaining accurate and reproducible kinetic results.

Quenching of ^{3}Zncyt by Cupriplastocyanin at Low Ionic Strength. The subscripts in the symbols for the intracomplex rate constants k_F (for the unimolecular reaction in eq 12) and k_f (for the bimolecular reaction in eq 13) are reminders

$$\text{Zncyt/pc(II)} \underset{k_d}{\overset{h\nu}{\rightleftharpoons}} {}^3\text{Zncyt/pc(II)} \xrightarrow{k_F} \text{Zncyt}^+\text{/pc(I)} \tag{12}$$

$$\text{Zncyt} + \text{pc(II)} \underset{k_d}{\overset{h\nu}{\rightleftharpoons}} {}^3\text{Zncyt} + \text{pc(II)} \underset{k_{off}}{\overset{k_{on}}{\rightleftharpoons}} {}^3\text{Zncyt/pc(II)} \xrightarrow{k_f} \text{Zncyt}^+\text{/pc(I)} \tag{13}$$

$$K_a = \frac{k_{on}}{k_{off}} \tag{14}$$

$$\Delta A = a_1 \exp(-k_F t) + a_2 \exp(-k_{obs} t) + b \tag{15}$$

that both of these are so-called forward reactions, defined above. We confirmed that the overall quenching is biphasic (that it has two components) at the ionic strengths of 2.5 and 10.0 mM for all cupriplastocyanin concentrations used and also at the ionic strength of 20.0 mM for the cupriplastocyanin concentrations of 20 μM or higher (Zhou & Kostić, 1991a). The rate constant k_F for the faster component, eq 12, is independent of cupriplastocyanin concentration in the entire temperature range examined. The rate constant k_{obs} for the slower component, eq 13, is dependent on the quencher concentration and shows saturation owing to association; the association constant is defined in eq 14. This behavior persists at all temperatures examined. The standard errors of fitting to eq 15 are as follows: 3−5% and 6−10%, respectively, for the amplitude (a_1) and the rate constant (k_F) of the faster component; 1−3% and 2−9%, respectively, for the amplitude (a_2) and the rate constant (k_{obs}) of the slower component; and 5−8% for the parameter *b*, which accounts for the natural decay and which was always less than 0.004.

Dependence of the Rate Constant k_F on Temperature. Temperature effects on the faster component, the unimolecular reaction in eq 12, were studied at ionic strengths of 2.5, 10.0, and 20.0 mM, at which this component has a relatively large relative amplitude; see Figure 1. The viscosity of these three buffers is independent (within the experimental error) of ionic strength, but somewhat dependent on temperature: 1.77, 1.80, and 1.82 cp, respectively, at 273.3 K; and 0.81, 0.85, and 0.90 cp, respectively, at 300.8

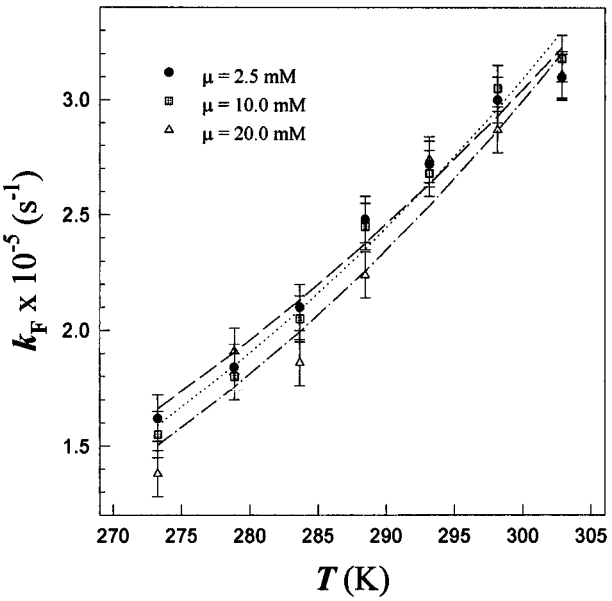

FIGURE 1: Temperature dependence of the rate constant k_F for the unimolecular component of the reaction between ^{3}Zncyt and pc-(II), shown in eq 12, in sodium phosphate buffers at pH 7.0 and three ionic strengths. The lines are fittings to eq 18. Because k_F is independent of ionic strength, points at some temperatures, and therefore also the lines, overlap.

K. This dependence, which might have complicated analysis of kinetic results, was eliminated in all subsequent experiments by adjusting the viscosity of the buffered solutions with sucrose. Different amounts of sucrose were added at each temperature, so that the viscosity was kept at 2.00, 4.00, 8.40, and 16.00 cp. Two series of experiments were performed, at ionic strengths of 2.5 mM (Figure 2a) and 10.0 mM (Figure 2b).

The results in Figure 2 were fitted to Arrhenius (eq 16) and Eyring (eqs 17 and 18) equations, in nonlinear (Figure 2) and linear (Supporting Information, Figure S2) forms. (The Boltzmann constant, k_B, should not be confused with the rate constants.) Nonlinear and linear fittings of each kind gave the same results, which are shown in Table 1.

$$k_F = A \exp\frac{-E_a}{RT} \quad (16)$$

$$k_F = \frac{k_B T}{h} \exp\frac{-\Delta G^{\ddagger}}{RT} \quad (17)$$

$$k_F = \frac{k_B T}{h} \exp\frac{\Delta S^{\ddagger}}{R} \exp\frac{-\Delta H^{\ddagger}}{RT} \quad (18)$$

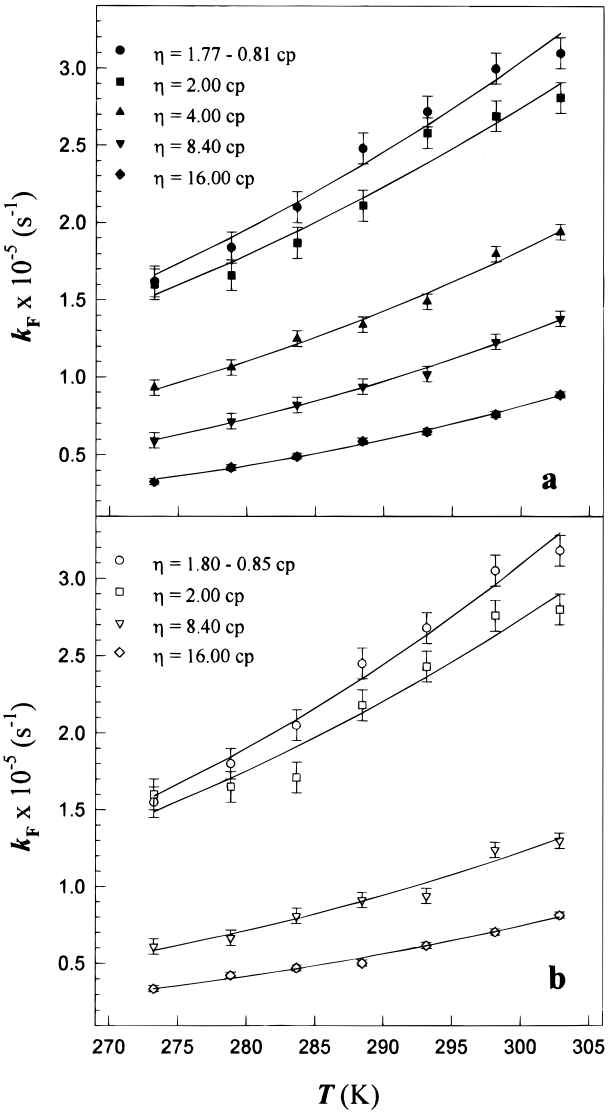

FIGURE 2: Temperature dependence of the rate constant k_F for the unimolecular component of the reaction between ^{3}Zncyt and pc-(II), shown in eq 12, in sodium phosphate buffers at pH 7.0 and ionic strengths of (a) 2.5 mM and (b) 10.0 mM. Because the viscosity of the buffer varies somewhat with temperature (the top plot at each ionic strength), the viscosity was maintained constant by addition of sucrose. The lines are fittings to eq 18; the same lines are obtained by fitting to eq 16.

Table 1: Dependence on Ionic Strength (μ) and Viscosity (η) of the Activation Parameters for the Unimolecular Reaction, Shown in Eq 12, Which Are Obtained by Fitting of the Observed Rate Constants k_F to the Equations Indicated

		eq 16		eq 17	eq 18	
μ (mM)	η^a (cp)	$A \times 10^{-7}$	E_a (kJ/mol)	$\Delta G^{\ddagger}$ (kJ/mol)	$\Delta H^{\ddagger}$ (kJ/mol)	$\Delta S^{\ddagger}$ (J/K mol)
2.5	1.77−0.81	15 ± 7	15 ± 1	41.6 ± 0.4	13 ± 2	−97 ± 4
	2.00	11 ± 7	15 ± 2	41.9 ± 0.4	12 ± 2	−99 ± 6
	4.00	21 ± 8	18 ± 1	42.9 ± 0.4	15 ± 1	−94 ± 3
	8.40	31 ± 9	19 ± 1	43.9 ± 0.3	17 ± 1	−90 ± 3
	16.00	58 ± 16	22 ± 1	45.0 ± 0.3	20 ± 1	−85 ± 3
10.0	1.80−0.85	28 ± 12	17 ± 1	41.6 ± 0.4	15 ± 1	−91 ± 4
	2.00	14 ± 10	16 ± 2	41.9 ± 0.4	13 ± 2	−97 ± 6
	8.40	24 ± 16	19 ± 2	44.0 ± 0.3	16 ± 2	−93 ± 6
	16.00	25 ± 10	20 ± 1	45.2 ± 0.3	18 ± 1	−92 ± 4
20.0	1.82−0.90	34 ± 26	18 ± 2	41.7 ± 0.4	15 ± 2	−90 ± 6

[a] Because viscosity of the pure buffers depends somewhat on temperature, ranges are given. In most experiments viscosity was kept constant with the additions of sucrose.

Dependence of the Rate Constant k_{obs} on Temperature at Low Ionic Strength. Temperature effects on the slower component, the reaction in eq 13, were also studied at ionic strengths of 2.5, 10.0, and 20.0 mM, at which this component has an increasing relative amplitude. The kinetic results were fitted to eq 15 iteratively. In the first round, both k_F and k_{obs} were variable parameters. Because the unimolecular rate constant k_F is independent of cupriplastocyanin concentration, in the second round it was justifiably fixed at the average k_F value at each temperature. Improved values of the bimolecular rate constant k_{obs} were thus obtained. Dependence of k_{obs} on the concentration of free cupriplastocyanin, designated [pc(II)], was fitted to eqs 19 and 20 and also to eqs 19a and 20a (Zhou & Kostić, 1991a). Equations 19a and

$$k_{obs} = \frac{k_{on}k_f[\text{pc(II)}]}{k_{off} + k_f + k_{on}[\text{pc(II)}]} \tag{19}$$

$$k_{obs} = \frac{k_{on}k_fK_a[\text{pc(II)}]}{k_{on} + k_fK_a + k_{on}K_a[\text{pc(II)}]} \tag{19a}$$

$$[\text{pc(II)}] = [\text{pc(II)}]_0 - \frac{1}{2}\left\{[\text{Zncyt}]_0 + [\text{pc(II)}]_0 + \frac{k_{off}}{k_{on}} - \sqrt{\left([\text{Zncyt}]_0 + [\text{pc(II)}]_0 + \frac{k_{off}}{k_{on}}\right)^2 - 4[\text{Zncyt}]_0[\text{pc(II)}]_0}\right\} \tag{20}$$

$$[\text{pc(II)}] = [\text{pc(II)}]_0 - \frac{1}{2}\left\{[\text{Zncyt}]_0 + [\text{pc(II)}]_0 + [\text{pc(II)}]_0 + K_a^{-1} - \sqrt{([\text{Zncyt}]_0 + [\text{pc(II)}]_0 + K_a^{-1})^2 - 4[\text{Zncyt}]_0[\text{pc(II)}]_0}\right\} \tag{20a}$$

20a are derived from eqs 19 and 20, respectively, and eq 14. The fitted values were obtained from the following pairs of equations: k_{on} and k_f, from eqs 19 and 20 and eqs 19a and 20a; k_{off} from eqs 19 and 20; and K_a from eqs 19a and 20a. The two fittings gave identical values. These fittings are shown in Supporting Information, Figure S3, and in Figure 3. The results are given in the top three-quarters of Tables 2 and 3, in which the standard errors of fitting are rounded conservatively. Two series of fittings, each with three parameters, were done first. One set was k_f, k_{on}, and k_{off}; the other was k_f, k_{on}, and K_a. Because the fitted values of k_f are equal, within the error margins, to the observed values of k_F over the entire temperature interval, improved fittings were possible. In them k_f was set equal to the more accurate k_F, so that the only variable parameters were k_{on} and k_{off} in one series of fittings and k_{on} and K_a in the other. The results of three-parameter fittings are shown in Table 2, and the results two-parameter fittings are shown in Table 3. The k_f values were fitted to eq 18, and the activation parameters $\Delta H^{\ddagger}$ and $\Delta S^{\ddagger}$ were obtained. The fittings to two parameters were better than fittings to three, and those at the ionic strengths of 20.0 and 10.0 mM were better than those at 2.5 mM.

Quenching of ^{3}Zncyt by Cupriplastocyanin at Intermediate Ionic Strength. We confirmed that this reaction is monophasic at the ionic strength of 30 mM and higher, regardless of the quencher concentration (Zhou & Kostić, 1991a). This

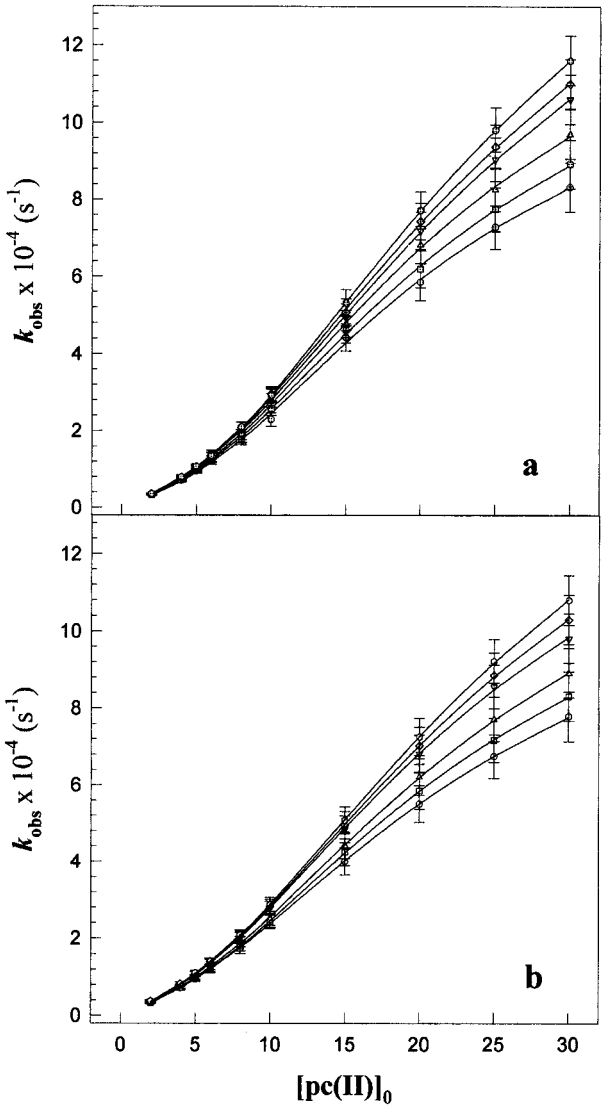

FIGURE 3: Temperature dependence of the rate constant k_{obs} for the bimolecular component of the reaction between ^{3}Zncyt and pc(II), shown in eq 13, in sodium phosphate buffers at pH 7.0 and ionic strengths of (a) 10.0 mM and (b) 20.0 mM. At each concentration of the quencher, cupriplastocyanin, k_{obs} increases as temperature increases in the order 273.3, 278.9, 283.7, 288.5, 293.2, and 298.2 K. The lines are fittings to eqs 19 and 20.

reaction is the same as the slower component at low ionic strength, eq 13. The standard errors of fitting to eq 21 are 1−3% for the amplitude a, 1−4% for the rate constant k_{obs}, and 9−20% for the parameter b, which was always less than 0.002.

$$\Delta A = a\exp(-k_{obs}t) + b \tag{21}$$

Dependence of the Rate Constant k_{obs} on Temperature at Intermediate Ionic Strength. The reaction in eq 13, which is the slower component at low ionic strength, is the only component at intermediate ionic strength. Temperature effects on this single component were studied at ionic strengths of 30 and 100 mM. This subsection, therefore, is related to the second subsection preceding this one. As before, the viscosity of the 30 and 100 mM buffers is independent (within the experimental error) of the ionic strength, but slightly dependent on temperature: 1.82 and 1.89 cp, respectively, at 273.3 K and 0.95 and 1.01 cp, respectively, at 300.8 K. We showed above this slight

Table 2: Microscopic Constants[a] for the Bimolecular Reaction, Shown in Eq 13, Which Are Obtained by Fittings of the Observed Rate Constants k_{obs} to Eqs 19 and 20 or to Eqs 19a and 20a, with Three Parameters

		fitting to eqs 19 and 20			fitting to eqs 19a and 20a		
μ (mM)	T (K)	$k_f \times 10^{-5}$ (s^{-1})	$k_{on} \times 10^{-9}$ (M^{-1} s^{-1})	$k_{off} \times 10^{-4}$ (s^{-1})	$k_f \times 10^{-5}$ (s^{-1})	$k_{on} \times 10^{-9}$ (M^{-1} s^{-1})	$K_a \times 10^{-5}$ (M^{-1})
2.5	273.3	1.8 ± 0.2	8.9 ± 0.4	1.0 ± 0.1	1.8 ± 0.2	8.9 ± 0.4	9.3 ± 0.5
	278.9	1.2 ± 0.1	11.5 ± 0.4	1.0 ± 0.1	1.2 ± 0.1	11.5 ± 0.4	11.8 ± 0.4
	283.7	2 ± 1	10 ± 2	1.0 ± 0.1	2 ± 1	10 ± 2	9 ± 2
	288.5	2 ± 1	10 ± 3	1.0 ± 0.1	2 ± 1	10 ± 3	10 ± 3
	293.2	6 ± 4	8.3 ± 0.9	1.0 ± 0.1	6 ± 4	8.3 ± 0.9	8 ± 1
	298.2	2 ± 1	11 ± 3	1.0 ± 0.1	2 ± 1	11 ± 3	11 ± 3
10.0	273.3	1.6 ± 0.2	9.0 ± 0.6	1.8 ± 0.2	1.6 ± 0.2	9.0 ± 0.6	5.1 ± 0.7
	278.9	1.8 ± 0.1	9.2 ± 0.4	1.8 ± 0.2	1.8 ± 0.1	9.2 ± 0.4	5.0 ± 0.5
	283.7	2.0 ± 0.2	9.6 ± 0.5	1.8 ± 0.2	2.0 ± 0.2	9.6 ± 0.5	5.2 ± 0.5
	288.5	2.6 ± 0.2	9.1 ± 0.4	2.0 ± 0.2	2.6 ± 0.2	9.1 ± 0.4	4.6 ± 0.5
	293.2	2.8 ± 0.2	9.3 ± 0.3	2.0 ± 0.1	2.8 ± 0.2	9.3 ± 0.3	4.6 ± 0.3
	298.2	3.1 ± 0.1	9.5 ± 0.1	2.0 ± 0.1	3.1 ± 0.1	9.5 ± 0.1	4.9 ± 0.1
20.0	273.3	1.6 ± 0.1	8.0 ± 0.3	2.1 ± 0.1	1.6 ± 0.1	8.0 ± 0.3	3.9 ± 0.3
	278.9	1.8 ± 0.1	8.3 ± 0.2	2.0 ± 0.1	1.8 ± 0.1	8.3 ± 0.2	4.3 ± 0.2
	283.7	2.0 ± 0.1	8.5 ± 0.2	2.0 ± 0.1	2.0 ± 0.1	8.5 ± 0.2	4.2 ± 0.2
	288.5	2.2 ± 0.1	9.3 ± 0.3	2.1 ± 0.1	2.2 ± 0.1	9.3 ± 0.3	4.4 ± 0.2
	293.2	2.5 ± 0.1	9.1 ± 0.2	2.1 ± 0.1	2.5 ± 0.1	9.1 ± 0.2	4.2 ± 0.2
	298.2	2.8 ± 0.1	9.0 ± 0.2	2.2 ± 0.1	2.8 ± 0.1	9.0 ± 0.2	4.2 ± 0.1
30	273.3	1.2 ± 0.3	1.7 ± 0.2	1.0 ± 0.2	1.2 ± 0.3	1.7 ± 0.2	1.8 ± 0.4
	278.9	1.5 ± 0.1	1.7 ± 0.1	1.2 ± 0.1	1.5 ± 0.1	1.7 ± 0.1	1.4 ± 0.1
	283.7	1.9 ± 0.2	1.8 ± 0.1	1.4 ± 0.1	1.9 ± 0.2	1.8 ± 0.1	1.3 ± 0.1
	288.5	1.9 ± 0.1	2.0 ± 0.1	1.4 ± 0.1	1.9 ± 0.1	2.0 ± 0.1	1.4 ± 0.1
	293.2	2.1 ± 0.2	2.1 ± 0.1	1.6 ± 0.1	2.1 ± 0.2	2.1 ± 0.1	1.3 ± 0.1
	298.2	2.8 ± 0.9	2.2 ± 0.6	1.7 ± 0.7	2.8 ± 0.9	2.2 ± 0.6	1.2 ± 0.8

[a] Listed errors are standard errors of fitting, given by SigmaPlot.

Table 3: Microscopic Constants[a] for the Bimolecular Reaction, Shown in Eq 13, Which Are Obtained by Fittings of the Observed Rate Constants k_{obs} to Eqs 19 and 20 or to Eqs 19a and 20a, with Two Parameters

		fitting to eqs 19 and 20		fitting to eqs 19a and 20a	
μ (mM)	T (K)	$k_{on} \times 10^{-9}$ (M^{-1} s^{-1})	$k_{off} \times 10^{-4}$ (s^{-1})	$k_{on} \times 10^{-9}$ (M^{-1} s^{-1})	$K_a \times 10^{-5}$ (M^{-1})
2.5	273.3	9.4 ± 0.1	1.0 ± 0.1	9.4 ± 0.1	9.8 ± 0.2
	278.9	9.1 ± 0.1	1.0 ± 0.1	9.1 ± 0.1	8.9 ± 0.3
	283.7	9.5 ± 0.2	1.0 ± 0.1	9.5 ± 0.2	9.4 ± 0.5
	288.5	9.6 ± 0.2	1.0 ± 0.1	9.6 ± 0.2	9.5 ± 0.5
	293.2	9.7 ± 0.1	1.0 ± 0.1	9.7 ± 0.1	9.8 ± 0.3
	298.2	9.9 ± 0.2	1.0 ± 0.1	9.9 ± 0.2	10.2 ± 0.6
10.0	273.3	9.2 ± 0.2	1.7 ± 0.2	9.2 ± 0.2	5.3 ± 0.4
	278.9	9.3 ± 0.1	1.8 ± 0.1	9.3 ± 0.1	5.1 ± 0.3
	283.7	9.4 ± 0.1	1.9 ± 0.1	9.4 ± 0.1	5.0 ± 0.3
	288.5	9.4 ± 0.1	1.9 ± 0.1	9.4 ± 0.1	4.9 ± 0.3
	293.2	9.5 ± 0.3	2.0 ± 0.1	9.5 ± 0.1	4.8 ± 0.2
	298.2	9.6 ± 0.1	1.9 ± 0.1	9.6 ± 0.1	5.0 ± 0.1
20.0	273.3	8.1 ± 0.1	2.0 ± 0.1	8.1 ± 0.1	4.0 ± 0.2
	278.9	8.2 ± 0.1	2.0 ± 0.1	8.2 ± 0.1	4.1 ± 0.1
	283.7	8.2 ± 0.1	2.1 ± 0.1	8.2 ± 0.1	3.9 ± 0.1
	288.5	8.5 ± 0.1	2.3 ± 0.1	8.5 ± 0.1	3.7 ± 0.2
	293.2	8.7 ± 0.1	2.3 ± 0.1	8.7 ± 0.1	3.8 ± 0.1
	298.2	8.7 ± 0.1	2.2 ± 0.1	8.7 ± 0.1	3.9 ± 0.1
30	273.3	1.6 ± 0.1	1.1 ± 0.1	1.6 ± 0.1	1.4 ± 0.2
	278.9	1.6 ± 0.1	1.3 ± 0.1	1.6 ± 0.1	1.3 ± 0.1
	283.7	1.7 ± 0.1	1.4 ± 0.1	1.7 ± 0.1	1.2 ± 0.1
	288.5	1.8 ± 0.1	1.6 ± 0.1	1.8 ± 0.1	1.2 ± 0.1
	293.2	2.0 ± 0.1	1.8 ± 0.1	2.0 ± 0.1	1.1 ± 0.1
	298.2	2.1 ± 0.1	1.8 ± 0.4	2.1 ± 0.1	1.2 ± 0.3

[a] Listed errors are standard errors of fitting, given by SigmaPlot.

dependence to be inconsequential, within the error margins of the kinetic experiments. At the ionic strength of 100 mM, at which the quenching is relatively slow, natural decay of the triplet state could not be neglected. Therefore k_d was subtracted from k_{obs}; the results are shown in Figure 4b. Saturation effects at low ionic strength (Figure 3) are absent at the ionic strength of 100 mM (Figure 4). Fittings of these results at the ionic strength of 30 mM to eqs 19 and 20 or to eqs 19a and 20a gave the microscopic rate constants and the association constants that are listed in the bottom quarters of Tables 2 and 3. The fittings were done as described above for the rate constant k_{obs} at low ionic strength; see the second subsection preceding this one. Again, fittings to two parameters were consistently better than fittings to three.

Dependence of the Rate Constant k_f on Temperature. This dependence at the ionic strengths of 10.0, 20.0, and 30 mM is shown in Figure 5. As the curvature owing to saturation becomes smaller, the data points become more disperse. For this reason, the data points at the ionic strength of 100 mM

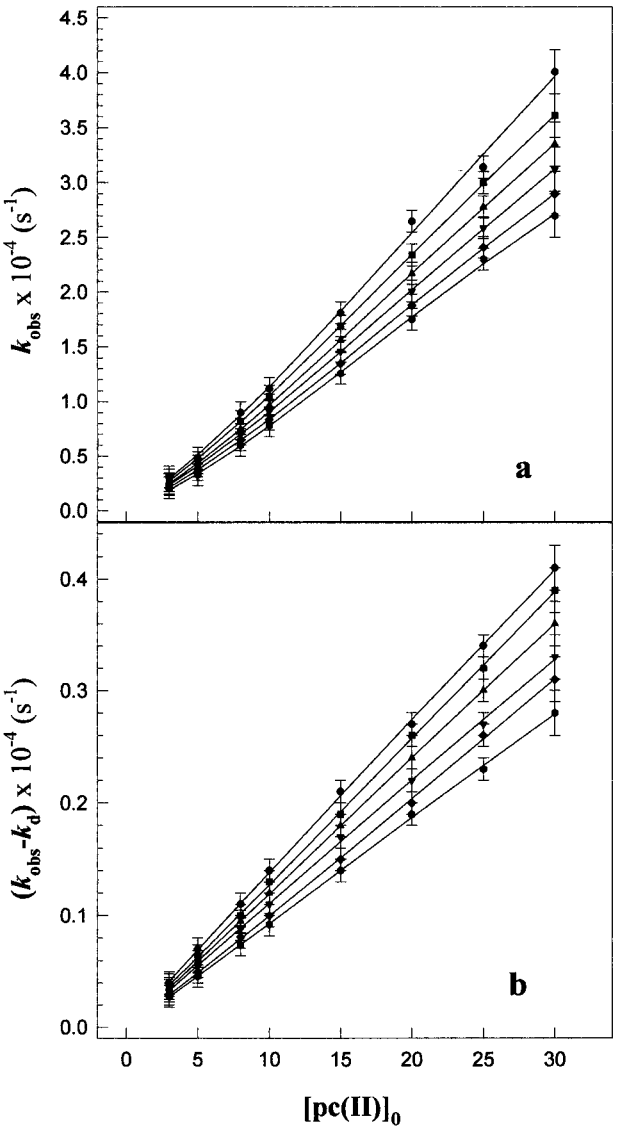

FIGURE 4: Temperature dependence of the rate constant k_{obs} for the bimolecular component of the reaction between ^{3}Zncyt and pc(II), shown in eq 13, in sodium phosphate buffers at pH 7.0 and ionic strengths of (a) 30 mM and (b) 100 mM. At each concentration of the quencher, cupriplastocyanin, k_{obs} increases as temperature increases in the order 273.3, 278.9, 283.7, 288.5, 293.2, and 298.2 K. The lines are fittings to eqs 19 and 20.

are not shown in Figure 5. Fittings to eq 18 yielded the activation parameters $\Delta H^{\ddagger}$ and $\Delta S^{\ddagger}$.

Dependence of the Relative Amplitudes on Temperature. Although the amplitudes, a_1 and a_2 in eq 15, are less accurate than the rate constants, their values at the ionic strengths of 2.5 and 10.0 mM were reliable enough to be analyzed. Fittings to eq 22 of the fractional contribution of the unimolecular component, $a_1/(a_1 + a_2)$, are shown in Supporting Information, Figure S4, and the residuals are shown in Figure S5. The results are given in Table 4. The lower the ionic strength, the greater the association constant (K_a) and the greater the relative amplitude (i.e., the contribution to the total reaction) of the unimolecular component.

$$\frac{a_1}{a_1 + a_2} = \frac{1}{2[\text{Zncyt}]_0}\Big\{[\text{Zncyt}]_0 + [\text{pc(II)}]_0 + K_a^{-1} - \sqrt{([\text{Zncyt}]_0 + [\text{pc(II)}]_0 + K_a^{-1})^2 - 4[\text{Zncyt}]_0[\text{pc(II)}]_0}\Big\} \quad (22)$$

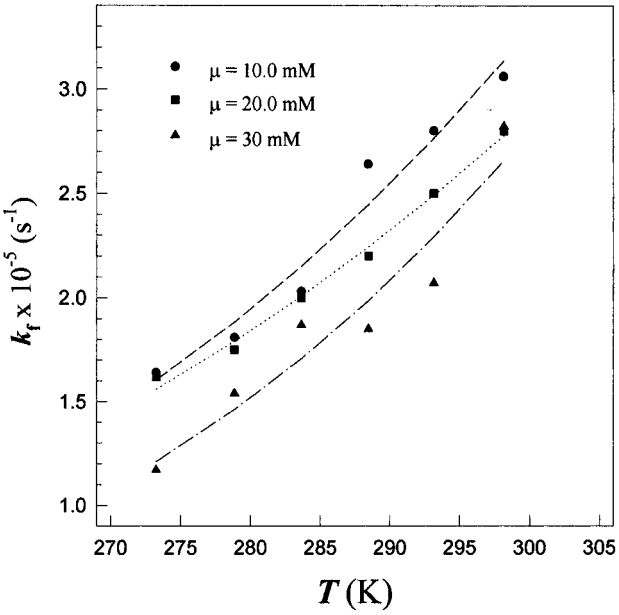

FIGURE 5: Temperature dependence of the unimolecular rate constant k_f for gated electron transfer within the encounter complex ^{3}Zncyt/pc(II), shown in eq 13, in sodium phosphate buffers at pH 7.0 and three ionic strengths. The standard errors of fitting to eqs 19 and 20 are given in Table 2. The lines are fittings to eq 18. The standard errors of fitting to eq 18 are given in the Discussion.

Error Margins. The results in Tables 2 and 3 at the ionic strengths of 10.0, 20.0, and 30 mM are more precise than those at 2.5 and 100 mM. The results at 20.0 mM are the most precise of all. The error bars shown in figures reflect the uncertainty of experiments, not merely of fittings. An error bar encloses all the results obtained in repetitions of a given experiment.

Protein Surface Areas. The results in Table 5 are internally consistent. The computed total surface area (A_{tot}) agreed very well with the sum of the computed hydrophobic (A_{phob}) and hydrophilic (A_{phil}) areas in each case. The difference between the sum of the surface areas of separate cytochrome *c* and plastocyanin and the surface area of a given configuration of the diprotein complex treated as a single molecule equaled the surface area buried at the protein−protein interface. As expected, the sum of the accessible and buried surfaces was virtually the same for all three configurations of the diprotein complex and equal to the sum of surface areas of the separate protein molecules. An example of consistency in the "horizontal" direction in Table 5 is the sum $554 + 636 \approx 1193$. An example in the "vertical" direction are the following values of A_{phil}, in Å^2: $4055 = 4055 \approx 4019 \approx 4058$; $4055 \approx 3501 + 552$; and $552 \approx 554$.

DISCUSSION

The Quenching Reaction and Its Two Components. Because zinc cytochrome *c* and cupriplastocyanin bear respective net charges of +6 and −8 at pH 7.0 and because they contain complementary surface patches, these two proteins associate in solution if the ionic strength is sufficiently low. Replacement of iron(II) with zinc(II) in the heme does not significantly perturb the surface of cytochrome *c* and its interactions with other proteins (Ye et al., 1997; Angiolillo & Vanderkooi, 1995; Anni et al., 1995; Moore et al., 1980). Much evidence shows that in the complexes cyt/pc and

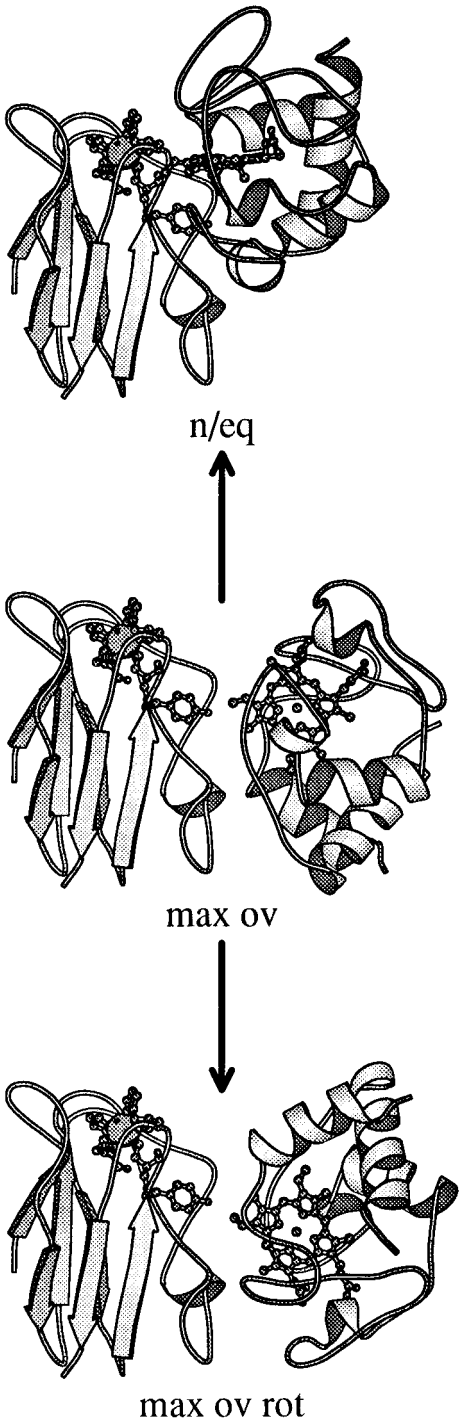

FIGURE 6: Three configurations of the complex between cytochrome *c* and plastocyanin, with original designations (Roberts et al., 1991). The arrows show the rearrangements analyzed in terms of the activation parameters $\Delta H^{\ddagger}$ and $\Delta S^{\ddagger}$. The upward arrow represents the process responsible for gating of the electron-transfer reactions within the persistent diprotein complex (k_F in eq 12), and within the transient diprotein complex (k_f in eq 13).

Zncyt/pc the positive patch around the exposed heme edge in cytochrome *c* interacts with the broad, negative patch in plastocyanin (King et al., 1985; Bagby et al., 1990; Roberts et al., 1991; Geren et al., 1983; Zhou et al., 1992).

This study confirms the results of previous studies of the effects of ionic strength on the forward reaction (eqs 12 and 13) at a single temperature (Zhou & Kostić, 1991a, 1992a, 1993b) and adds to them an analysis of temperature effects and of activation parameters. The kinetic model was proven correct by thorough experiments at a single temperature (Zhou & Kostić, 1991a). The reaction is biphasic at the low ionic strength ($\mu \leq 20.0$ mM) and monphasic at intermediate and high ionic strength ($\mu \geq 30$ mM). The faster component is the unimolecular electron-transfer reaction (eq 12) within the preformed diprotein complex, Zncyt/pc, which exists prior to the laser flash. The unimolecular rate constant k_F is determined directly. The slower component at the low ionic strength, and the only one at the intermediate and high ionic strength, is the bimolecular electron-transfer reaction (eq 13), in which the triplet state ^{3}Zncyt forms an encounter complex with cupriplastocyanin, ^{3}Zncyt/pc(II). The composite rate constant k_{obs} is analyzed in terms of eqs 19 and 20 and eqs 19a and 20a to yield the unimolecular rate constant, k_f, for the reaction within the encounter complex.

Table 4: Temperature Dependence at Two Ionic Strengths (μ) of the Association Constant K_a for Zinc Cytochrome *c* and Cupriplastocyanin, Obtained by Fitting to Eq 22 the Relative Amplitudes of the Unimolecular (a_1) and Bimolecular (a_2) Components of the Quenching Reaction

	$K_a \times 10^{-4}$ (M^{-1})	
T (K)	$\mu = 2.5$ mM	$\mu = 10.0$ mM
273.3	90 ± 30	20 ± 5
278.9	90 ± 30	25 ± 5
283.7	70 ± 30	18 ± 4
288.5	50 ± 10	14 ± 2
293.2	50 ± 10	12 ± 2
298.2	40 ± 20	8 ± 2

Table 5: Surface Areas (in Å^2) for Cytochrome *c*, Plastocyanin, and Three Configurations of the Flexible Diprotein Complex cyt/pc

surface	proteins and configurations[a]	A_{phil}	A_{phob}	A_{tot}
total	cyt	1971	3714	5685
	pc	2084	2925	5010
	cyt + pc	4055	6640	10695
	max ov	4055	6639	10695
	max ov rot	4019	6672	10691
	n/eq	4058	6645	10702
accessible	max ov	3501	6003	9502
	max ov rot	3538	6005	9544
	n/eq	3501	5909	9410
buried	max ov	552	638	1190
	max ov rot	482	658	1140
	n/eq	552	733	1286
total − accessible	max ov	554	636	1193
	max ov rot	481	667	1147
	n/eq	557	736	1292

[a] The three configurations are designated after Roberts et al. (1991).

Outline of the Discussion. In the following subsections we will first explain how activation parameters were obtained by analyzing the dependence of k_F and k_f on temperature. Then we will compare the preformed and the encounter complexes ^{3}Zncyt/pc(II) by comparing the respective rate constants k_F and k_f and the corresponding activation parameters. We will briefly comment on the magnitudes of the activation parameters and on their dependence on viscosity and will propose explanations of these magnitudes. Then we will state our assumptions, analyze energetics of protein association, and build on this analysis the interpretation of the activation parameters for the rearrangement of the diprotein complex.

Dependence of the Rate Constant k_F on Temperature. Because the rate constant k_F depends on viscosity, which in

turn depends on temperature, changes in temperature could, in principle, affect k_F both directly and indirectly. To avoid complications, we kept viscosity constant by adding to the reaction mixture different amounts of a buffered sucrose solution at different temperatures. The values of $k_F \times 10^{-5}$ at the ionic strength of 2.5 mM and at the six (increasing) temperatures listed in Table 2 are 1.6, 1.8, 2.1, 2.5, 2.7, and 3.0 s^{-1}.

As Figures 1 and 2 and Figure S2 in the Supporting Information show, k_F is independent of ionic strength, within the error margins of the experiments. The quality of fitting in Figure 1 is evident from the residuals in Supporting Information, Figure S6. As the values of K_a in Tables 2 and 3 show, ionic strength affects the degree of protein association, i.e., the concentration of the diprotein complex. Ionic strength, however, does not seem to affect the electron-transfer properties of this complex, even though it is clearly a dynamic system. In studies of various protein pairs the dependence of the observed rate constant on ionic strength, sometimes at only two values of it, has been taken as evidence for rearrangement of the protein complex (Kostić, 1991). This reasoning may be correct in particular cases, but intuitive equating of stability and rigidity is ambiguous. Position of an equilibrium between free proteins and their complex is a matter of thermodynamics, whereas the rate at which this equilibrium is established and the rate at which the complex may rearrange are matters of kinetics.

The Arrhenuis parameters, A and E_a, are less useful than the Eyring parameters, $\Delta S^{\ddagger}$ and $\Delta H^{\ddagger}$. They are related by eqs 23 and 24. These equations apply to the corresponding

$$\Delta S^{\ddagger} = R \ln \frac{Ah}{eTk_B} \tag{23}$$

$$\Delta H^{\ddagger} = E_a - RT \tag{24}$$

values in the same row in Table 1. Because $\Delta G^{\ddagger}$ depends on temperature, fitting to eq 17, with one parameter, is inadequate. Therefore fitting to eq 18, with the activation parameters $\Delta H^{\ddagger}$ and $\Delta S^{\ddagger}$, is justified. Indeed, these two quantities are virtually independent of temperature. The results are shown in Table 1 and will be analyzed near the end of the article.

Dependence of the Rate Constant k_f on Temperature. Activation parameters for the bimolecular reaction in eq 13 were reliably determined at the ionic strengths of 10.0, 20.0, and 30 mM; see Figure 5 and the resuduals in Supporting Information, Figure S7. The respective values of $\Delta H^{\ddagger}$ are 16 ± 2, 13 ± 1, and 19 ± 4 kJ/mol. The respective values of $\Delta S^{\ddagger}$ are -87 ± 7, -96 ± 3, and -77 ± 12 J/K mol. Within the error margins, these values are equal to those in Table 1, obtained from the unimolecular rate constants k_F. This equality, and the aforementioned equality of the rate constants k_F and k_f, confirm that the preformed and the encounter complex ^{3}Zncyt/pc(II) have identical electron-transfer properties. Most likely, these two complexes are the same. The two protein molecules associate in the same way in the persistent and the transient complex, and in both complexes electron transfer is gated by a rearrangement.

Values of the Activation Parameters. We have the activation parameters $\Delta H^{\ddagger}$ and $\Delta S^{\ddagger}$ (and can calculate $\Delta G^{\ddagger}$ from them) at several ionic strengths. Because the values obtained from k_F (Figures 1, 2, and S2) and from k_F (Figure 5) at the same ionic strength are equal, we can use the values from either set. For the best accuracy, however, we base the discussion below on the values obtained (by fitting to eq 18) from the rate constants for that reaction that has the larger amplitude at the particular ionic strength. At 2.5 mM, it is the unimolecular reaction (the faster component), whose rate constant is k_F. At 30 mM, it is the bimolecular reaction (the single component), whose rate constant is k_f. Since the plots in Figure 4b are linear, activation parameters at the ionic strength of 100 mM are unavailable. Even the plots in Figure 4a, obtained at 30 mM, are only slightly curved. This near linearity makes fitting worse and k_f values more disperse, as can be seen in Figure 5 for the data points at the ionic strength of 30 mM. Only the curved lines in Figure 3 justify using eq 19, as has been discussed in detail earlier (Zhou & Kostić, 1991a). At the ionic strengths of 10.0 and 20.0 mM, values from either set can reliably be used.

Dependence of Activation Parameters on Viscosity. As Table 1 shows, with increasing viscosity $\Delta H^{\ddagger}$ increases, whereas $\Delta S^{\ddagger}$ remains constant or slightly increases (becomes less negative). The change in activation parameters with viscosity is shown in Supporting Information, Table S1. The change in $\Delta H^{\ddagger}$ retards the reaction, whereas the change in $\Delta S^{\ddagger}$ does not affect or slightly assists the reaction. Since the rate constant decreases as viscosity of the solution increases, the change in $\Delta H^{\ddagger}$ is the dominant factor, responsible for the slowing down of the protein rearrangement (Zhou & Kostić, 1992a, 1993b; Qin & Kostić, 1994). This finding throws new light on the gated electron-transfer reaction in eqs 3 and 5 and possibly on similar reactions involving other protein pairs.

Configurations of the Diprotein Complex. We consider the three most realistic configurations of the electrostatic complex between cytochrome *c* and plastocyanin, those designated maximum-overlap (max ov); maximum-overlap, rotated (max ov rot); and northern equatorial (n/eq) in the original theoretical study (Roberts et al., 1991). (We retain these designations, for clarity.) The first configuration provides optimal electrostatic interactions (Roberts et al., 1991), but the latter two provide more efficient paths for electron transfer from the heme to the copper site (Ullmann & Kostić, 1995). Indeed, there is clear experimental evidence that the diprotein complex rearranges from the optimal docking configuration (Zhou & Kostić, 1992a, 1993b). Replacement of iron(II) by zinc(II) in the heme group does not detectably perturb the conformation of cytochrome *c* and its interaction with other proteins (Anni et al., 1995; Ye et al., 1997; Moore et al., 1980). Electronic excitation of zinc cytochrome *c* can not alter the geometric structure of this protein and its association with plastocyanin. It is, therefore, safe to assume that the complexes Zncyt/pc and ^{3}Zncyt/pc have identical structures. The actual structure of the transition state for the rearrangement of ^{3}Zncyt/pc(II) that gates the reaction in eq 3 is, of course, unknowable. We have available three configurations, shown in Figure 6, and we reasonably assign max ov to be the initial docking configuration. We then use the max ov rot and n/eq configurations as two models for the transition state in the rearrangement of the complex ^{3}Zncyt/pc(II). Under these assumptions, the difference in G, H, or S between the max ov and another configuration would be the $\Delta G^{\ddagger}$, $\Delta H^{\ddagger}$, or $\Delta S^{\ddagger}$ for the rearrangement.

Energetics of Protein Association. Now we consider the second equilibrium in eq 13. The K_a values in Tables 2 and 3 are more accurate than those in Table 4, for two reasons. First, the rate constant k_{obs} is known more accurately than the relative amplitude $a_1/(a_1+a_2)$. Second, fitting of k_{obs} to eqs 19 and 20 (or 19a and 20a) is more accurate than fitting of the relative amplitude to eq 22. The two methods of obtaining K_a are not independent, because they are based on different results of the same kinetic experiments. Nevertheless, the good agreement between the two series of K_a values, especially at the lowest ionic strength and at lower temperatures, is reassuring.

The free-energy change (ΔG) was calculated from eq 25 at each ionic strength. The values range from −30 kJ/mol

$$\Delta G = -RT \ln K_a \tag{25}$$

$$\Delta G = \Delta H - T\Delta S \tag{26}$$

at 2.5 mM to −20 kJ/mol at 100 mM. Plots of these values versus temperature according to eq 26, which are not shown, yielded a relatively inaccurate intercept (ΔH) and a more accurate slope, $\Delta S \approx 100$ J/K mol. This value is similar to those reported recently for pairs of redox metalloproteins (Harris & Davidson, 1993; Mauk et al., 1994; Kresheck et al., 1995).

This analysis of protein association is an approximate one. A detailed treatment of a diprotein complex requires massive calculations. In thorough molecular-dynamics simulations water must be explicitly included, and the proteins must be allowed conformational flexibility. Only then can the structures of the diprotein complex and the energetics of association be analyzed in detail. Such a study, the first of its kind, has recently been done with cytochrome *f* and plastocyanin (Ullmann et al., in press). Until such detailed calculations become more practicable, simpler analyses as in this and other recent studies will continue to be useful.

Energetics of Protein Rearrangement. We will now attempt to explain the activation parameters for the rate-limiting rearrangement, which we showed above to be the same for the preformed and the encounter complexes ^{3}Zncyt/pcII. We will try to account for the values $\Delta H^{\ddagger} = 13$ kJ/mol and $\Delta S^{\ddagger} = -97$ J/K mol, in the first row in Table 1.

Because these two protein molecules are relatively rigid, the enthalpy of activation probably is not caused by significant changes in their conformations. It probably is caused mostly by changes in solvation that accompany the rearrangement of the two associated proteins with respect to each other.

From studies of protein oligomerization (Weber, 1993) emerged an empirical method, embodied in eqs 27 and 28, for calculating enthalpy of protein association, ΔH, from enthalpies of protein−protein, water−water, and protein−water interactions. The corresponding parameters are,

$$\Delta H = (\Delta H_{pp} + \Delta H_{ww} - 2\Delta H_{pw})_n \tag{27}$$

$$n = \frac{\Delta A_{tot}}{10\ \text{Å}^2} \tag{28}$$

respectively, −3.18, −29.3, and −16.1 kJ/mol (Weber, 1993). The quantity ΔH is proportional to the number (n) of water molecules, each having a surface area of 10 Å^2, that become excluded from the interface upon complex formation. The results in Table 6 agree with the computational study (Roberts et al., 1991), which showed the configurations to have nearly identical energies of electrostatic stabilization, within ca. 3 kJ/mol. This finding, however, cannot explain the value of $\Delta H^{\ddagger}$ because a barrier of 13 kJ/mol between nearly isoenergetic configurations is unlikely. This empirical method did not discriminate among the three configurations, possibly because it is based on considerations of total buried surface, ΔA_{tot} in eq 28.

Table 6: Surface Areas Buried upon Formation of Three Configurations of the Complex cyt/pc and Enthalpies of Association Calculated from Them

cyt/pc configuration	ΔA_{tot} (Å^2)	ΔH (kJ/mol)
max ov	1190	−39.7
max ov rot	1140	−38.1
n/eq	1286	−43.1

A more detailed analysis requires consideration of changes in hydrophilic (polar) and hydrophobic (nonpolar) surfaces upon protein association. Contributions to thermodynamic functions from the removal of polar and nonpolar surfaces from water is an important issue in analysis of protein folding (Spolar et al., 1992; Spolar & Record, 1994). The empirical method in eqs 29−31, in which the factor 4.2 converts from cal into J units, has proven successful. This method was

$$\Delta C_p = 4.2(-0.45\Delta A_{phobic} + 0.26\Delta A_{philic}) \tag{29}$$

$$\Delta H = 4.2(35\Delta A_{philic}) + (373 - T)\Delta C_p \tag{30}$$

$$\Delta S = 1.35\Delta C_p \ln(T/386) \tag{31}$$

used to analyze reactions between proteins, including some redox metalloproteins (Murphy & Freire, 1992; Kresheck et al., 1995; Jelesarov & Bosshard, 1994).

We carried the analysis one step further. We applied eqs 29−31 to the data in Table 5 and calculated ΔH and ΔS for protein association in three configurations. Then we assumed that a difference between the values of a given thermodynamic parameter for two configurations is related to the corresponding activation parameter for the rearrangement of one configuration into the other. The results are given in Table 7. The top three values of ΔH indicate that the three configurations have similar enthalpies, but that the one designated max ov is somewhat more stable than the other two. Considering the different methods used in this analysis and in the previous analysis of electrostatic interactions (Roberts et al., 1991), the semiquantitative agreement between the findings is noteworthy.

According to our model, ΔH and ΔS for the two rearrangements shown on the bottom of Table 7 correspond to the experimental values of $\Delta H^{\ddagger}$ and $\Delta S^{\ddagger}$. The value $\Delta H = 13$ kJ/mol in Table 7 is equal to the value of $\Delta H^{\ddagger}$ for the gating process. We conclude that the rearrangement of the max ov configuration, or of another similar to it, possibly proceeds via the n/eq configuration, or another similar to it, as a transition state.

Both rearrangements in Table 7 result in burial of hydrophobic surfaces, a change that raises the entropy of the protein pair. Hence the two positive ΔS values on the bottom of Table 7.

The fact that $\Delta S^{\ddagger}$ is negative can be explained in terms of the structural properties of the cyt/pc complex. Besides the

Table 7: Protein Association (Top Three Rows) and Complex Rearrangement (Bottom Two Rows): Surface Areas Buried or Changed, and Thermodynamic Parameters Calculated from Them

process	configuration(s)	ΔA_{phil} (Å^2)	ΔA_{phob} (Å^2)	ΔC_p (J/K mol)	ΔH (kJ/mol)	ΔS (J/K mol)
association cyt + pc → cyt/pc	max ov	552	638	−602	−34.5	222
	max ov rot	482	658	−715	−16.9	264
	n/eq	552	733	−774	−22.8	285
rearrangement (cyt/pc) → (cyt/pc)*	max ov → max ov rot	−70	21	−113	18.7	42
	max ov → n/eq	0	95	−172	13.0	63

aforementioned electrostatic modeling (Roberts et al., 1991) and the approximate thermodynamic quantities in Tables 6 and 7, there is NMR spectroscopic evidence that these two protein molecules form a loose complex. On the NMR time scale, no plastocyanin residues are hidden from $[Cr(NH_3)_6]^{3+}$ by association with cytochrome *c* (Bagby et al., 1990). Because electron transfer through solvent or through space is unfavorable, the protein molecules must establish a more intimate contact, i.e., form a more compact complex. This tightening is reflected in the negative value of $\Delta S^{\ddagger}$ for the gating process.

If our model is correct, burying of the hydrophobic surface as the initial complex reaches a transition state would make a positive contribution to $\Delta S^{\ddagger}$, amounting to 42 or 63 J/K mol (from Table 7). It is the negative contribution from the aforementioned tightening that results in the experimental value of $\Delta S^{\ddagger} = -97$ J/K mol.

This explanation agrees well with the results of the aforementioned detailed theoretical study of the complex that plastocyanin forms with cytochrome *f* (Ullmann et al., in press). This complex (Qin & Kostić, 1993) is very similar in kinetic terms to the complex with cytochrome *c*, the subject of this study. In both of them, electron-transfer reaction requires a rearrangement. In the configuration providing the highest binding affinity plastocyanin and cytochrome *f* are farther apart than in the configuration providing the best electronic coupling of the heme and the copper site. As former rearranges into the latter, one protein partially rotates and closely approaches the other (Ullmann et al., in press). This is exactly a tightening of the kind proposed in this experimental study.

CONCLUSION

The photoinduced electron-transfer reaction between zinc cytochrome *c* and cupriplastocyanin is gated at all temperatures and viscosities examined. The persistent diprotein complex formed at low ionic strength and the transient complex formed by protein encounter at higher ionic strength are identical or very similar to each other. Although these complexes are dynamic, both the rate constant and the activation parameters $\Delta H^{\ddagger}$ and $\Delta S^{\ddagger}$ are independent of ionic strength (in the interval examined). This result is a reminder that changes in ionic strength do not necessarily affect the flexibility of protein complexes. Enthalpy of activation reflects a change in the character of the exposed surface as the diprotein complex rearranges. The same change would contribute positively to entropy of activation, but the negative contributions dominate. Entropy of activation may reflect tightening of the contact between the associated proteins. The quantity $\Delta H^{\ddagger}$ was reproduced by an empirical method. The conclusion about $\Delta S^{\ddagger}$ agrees with a detailed theoretical analysis of a very similar diprotein complex. According to our study, the so-called maximum-overlap (max ov) configuration, or a similar one, provides for optimal docking, whereas a configuration similar to the so-called northern equatorial (n/eq) provides for optimal electron transfer.

ACKNOWLEDGMENT

We thank G. Matthias Ullmann for Figure 6 and consultations and Drs. Elizabeth D. Getzoff and Victoria A. Roberts for atomic coordinates as in Roberts et al., 1991.

SUPPORTING INFORMATION AVAILABLE

One table showing the viscosity dependence of $\Delta G^{\ddagger}$, $\Delta H^{\ddagger}$, and $\Delta S^{\ddagger}$; four figures showing temperature dependence of k_d, k_F, k_{obs}, and $a_1/(a_1 + a_2)$; and three figures showing residuals for fitting of $a_1/(a_1 + a_2)$, k_F, and k_f (8 pages). Ordering information is given on any current masthead page.

REFERENCES

Angiolillo, P. J., & Vanderkooi, J. M. (1995) *Biophys. J. 68*, 2505.
Anni, H., Vanderkooi, J. M., & Mayne, L. (1995) *Biochemistry 34*, 5744.
Bagby, S., Driscoll, P. C., Goodall, K. G., Redfield, C., & Hill, H. A. O. (1990) *Eur. J. Biochem. 188*, 413.
Barber, E. J. (1966) *Natl. Cancer Inst. Monogr. 21*.
Brunschwig, B. S., & Sutin, N. (1989) *J. Am. Chem. Soc. 111*, 7454.
Burch, A. M., Rigby, S. E. J., Funk, W. D., MacGilliwray, R. T. A., Mauk, M. R., Mauk, A. G., & Moore, G. R. (1990) *Science 247*, 831.
Chen, L., Poliks, R., Hamada, K., Chen, Z., Mathews, F. S., Davidson, V. L., Satow, Y., Huizinga, E., Vellieux, F. M. D., & Hol, W. G. J. (1992) *Biochemistry 31*, 4959.
Chen, L., Durley, R. C. E., Mathews, F. S., & Davidson, V. L. (1994) *Science 264*, 86.
Connolly, M. L. (1983) *Science 221*, 709.
CRC Handbook of Biochemistry and Molecular Biology, 3rd ed. (1975) CRC Press, Cleveland, OH.
Fietelson, J., & McLendon, G. (1991) *Biochemistry 30*, 5051.
Geren, L. M., Stonehuerner, J., Davies, D. J., & Millett, F. (1983) *Biochim. Biophys. Acta 724*, 62.
Gross, E. L. (1993) *Photosynth. Res. 37*, 103.
Guss, J. M., & Freeman, H. C. (1983) *J. Mol. Biol. 169*, 521.
Harris, T. K., & Davidson, V. L. (1993) *Biochemistry 32*, 14145.
Harris, T. K., Davidson, V. L., Chen, L., Mathews, F. S., & Xia, Z.-X. (1994) *Biochemistry 33*, 12600.
Hoffman, B. M., & Ratner, M. A. (1987) *J. Am. Chem. Soc. 109*, 6237.
Hoffman, B. M., & Ratner, M. A. (1988) *J. Am. Chem. Soc. 110*, 8267.
Hoffman, B. M., Ratner, M. A., & Wallin, S. A. (1990) *Adv. Chem. Ser. 226*, 125.
Hoffman, B. M., Natan, M. J., Nocek, J. M., & Wallin, S. A. (1991) *Struct. Bond. 75*, 86.
ISCO Tables, 8th ed. (1982) ISCO, Lincoln, NE.
Jelesarov, I., & Bosshard, H. R. (1994) *Biochemistry 33*, 13321.
King, J. C., Binstead, R. A., & Wright, P. E. (1985) *Biochim. Biophys. Acta 106*, 262.
Kostić, N. M. (1991) *Met. Ions Biol. Syst. 27*, 129.
Kostić, N. M. (1996) in *Metal-Containing Polymeric Materials* (Pitman, C. U., Jr., et al., Eds.) p 491, Plenum, New York.

Kresheck, G. C., Vitello, L. B., & Erman, J. E. (1995) *Biochemistry 34*, 8398.
Mauk, A. G. (1991) *Struct. Bond. 75*, 131.
Mauk, M. R., Ferrer, J. C., & Mauk, A. G. (1994) *Biochemistry 33*, 12609.
McLendon, G. (1991a) *Struct. Bond. 75*, 160.
McLendon, G. (1991b) *Met. Ions Biol. Syst. 27*, 183.
McLendon, G., & Hake, R. (1992) *Chem. Rev. 92*, 481.
McLendon, G., Zhang, Q., Wallin, S. A., Miller, R. M., Billestone, W., Spears, K. G., & Hoffman, B. M. (1993) *J. Am. Chem. Soc. 115*, 3665.
Meyer, T. E., Zhao, C. G., Cusanovich, M. A., & Tollin, G. (1993) *Biochemistry 32*, 4552.
Milne, P. R., & Wells, J. R. E. (1970) *J. Biol. Chem. 245*, 1566.
Modi, S., He, S., Gray, J. C., & Bendall, D. S. (1992a) *Biochim. Biophys. Acta 1101*, 64.
Modi, S., Nordling, M., Lundberg, L. G., Hansson, O., & Bendall, D. S. (1992b) *Biochim. Biophys. Acta 1102*, 85.
Moore, G. R., & Pettigrew, G. W. (1990) *Cytochrome c: Evolutionary, Structural, and Physiochemical Aspects*, Springer Verlag, Berlin.
Moore, G. R., Williams, R. J. P., Chien, J. C. W., & Dickinson, L. C. (1980) *J. Inorg. Biochem. 13*, 1.
Murphy, K. P., & Freire, E. (1992) *Adv. Protein Chem. 43*, 313.
Nocek, J. M., Stemp, E. D. A., Finnegan, M. G., Koshy, T. I., Johnson, M. K., Margoliash, E., Mauk, A. G., Smith, M., & Hoffman, B. M. (1991) *J. Am. Chem. Soc. 113*, 6822.
Northrup, S. H., Boles, J. O., & Reynolds, J. C. L. (1988) *Science 241*, 67.
Peerey, L. M., & Kostić, N. M. (1989) *Biochemistry 28*, 1861.
Peerey, L. M., Brothers, H. M., II, Hazzard, J. T., Tollin, G., & Kostić, N. M. (1991) *Biochemistry 30*, 9297.
Pelletier, H., & Kraut, J. (1992) *Science 258*, 1748.
Pettigrew, G. W., & Moore, G. R. (1987) *Cytochrome c: Biological Aspects*, Springer-Verlag, Berlin.
Qin, L., & Kostić, N. M. (1992) *Biochemistry 31*, 5145.
Qin, L., & Kostić, N. M. (1993) *Biochemistry 32*, 6273.
Qin, L., & Kostić, N. M. (1994) *Biochemistry 33*, 12592.
Qin, L., & Kostić, N. M. (1996) *Biochemistry 35*, 3379.
Reddinbo, M. R., Yeates, T. O., & Merchant, S. (1994) *J. Bioenerg. Biomembr. 26*, 49.
Roberts, W. A., Freeman, H. C., Getzoff, E. D., Olson, A. J., & Tainer, J. A. (1991) *J. Biol. Chem. 266*, 13431.
Rodgers, K. K., Pochapsky, T. C., & Sligar, S. G. (1988) *Science 240*, 1657.
Scott, R. A., & Mauk, A. G., Eds. (1996) *Cytochrome c: A Multidisciplinary Approach*, University Science Books, Sausalito, CA.
Spolar, R. S., & Record, M. T., Jr. (1994) *Science 263*, 777.
Spolar, R. S., Livingstone, J. R., & Record, M. T., Jr. (1992) *Biochemistry 31*, 3947.
Sullivan, E. P., Jr., Hazzard, J. T., Tollin, G., & Enemark, J. H. (1992) *J. Am. Chem. Soc. 114*, 9662.
Sykes, A. G. (1991a) *Adv. Inorg. Chem. 36*, 377.
Sykes, A. G. (1991b) *Struct. Bond. 75*, 177.
Takano, T., & Dickerson, R. E. (1981) *J. Mol. Biol. 153*, 79.
Therien, M. J., Chang, J., Raphael, A. L., Bowler, B. E., & Gray, H. B. (1991) *Struct. Bond. 75*, 110.
Ullmann, G. M., & Kostić, N. M. (1995) *J. Am. Chem. Soc. 117*, 4766.
Ullmann, G. M., Knapp, E.-W., & Kostić, N. M. *J. Am. Chem. Soc.*, in press.
Vanderkooi, J. M., & Erecińska, M. (1975) *Eur. J. Biochem. 60*, 199.
Vanderkooi, J. M., Adar, F., & Erecińska, M. (1976) *Eur. J. Biochem. 64*, 381.
Walker, M. C., & Tollin, G. (1992) *Biochemistry 31*, 2798.
Wallin, S. A., Stemp, E. D. A., Everest, A. M., Nocek, J. M., Netzel, T. L., & Hoffman, B. M. (1991) *J. Am. Chem. Soc. 113*, 1842.
Weast, R. C., Ed. *CRC Handbook of Chemistry and Physics*, 66th ed., (1986) CRC Press, Boca Raton, FL.
Weber, G. (1993) *J. Phys. Chem. 97*, 7108.
Wendoloski, J. J., Matthew, J. B., Webber, P. C. & Salemme, F. R. (1987) *Science 238*, 794.
Willie, A., Steyton, P. S., Sligar, S. G., Durham, B., & Millett, F. (1992) *Biochemistry 31*, 7237.
Winkler, J. R., & Gray, H. B. (1992) *Chem. Rev.* 92, 369.
Ye, S., Shen, C., Cotton, T. M., & Kostić, N. M. (1997) *J. Inorg. Biochem.* (in press).
Zhou, J. S., & Kostić, N. M. (1991a) *J. Am. Chem. Soc. 113*, 6067.
Zhou, J. S., & Kostić, N. M. (1991b) *J. Am. Chem. Soc. 113*, 7040.
Zhou, J. S., & Kostić, N. M. (1992a) *J. Am. Chem. Soc. 114*, 3562.
Zhou, J. S., & Kostić, N. M. (1992b) *Biochemistry 31*, 7543.
Zhou, J. S., & Kostić, N. M. (1992c) *Spectrum 5* (2), 1.
Zhou, J. S., & Kostić, N. M. (1993a) *Biochemistry 32*, 4539.
Zhou, J. S., & Kostić, N. M. (1993b) *J. Am. Chem. Soc. 115*, 10796.
Zhou, J. S., & Hoffman, B. M. (1994) *Science 265*, 1693.
Zhou, J. S., Brothers, H. M., II, Neddersen, J. P., Peerey, L. M., Cotton, T. M., & Kostić, N. M. (1992) *Bioconjugate Chem. 3*, 382.
Zhou, J. S., Nocek, J. M., DeVan, M. L., & Hoffman, B. M. (1995) *Science 269*, 204.

BI961608G